blood
Leading the world in reporting basic and applied hematology research
JOURNAL OF THE AMERICAN SOCIETY OF HEMATOLOGY
Original Article | Current Issue | About Blood | Submissions | Subscriptions | Contact Us

Blood. 2018 Jan 18; 131(3): 342–352.
Prepublished online 2017 Oct 26.
doi: 10.1182/blood-2017-02-768580: 10.1182/blood-2017-02-768580
PMCID: PMC5774206
PMID: 29074498

Ferritin is secreted via 2 distinct nonclassical vesicular pathways

Marianna Truman-Rosentsvit,[1] Dina Berenbaum,[1] Lior Spektor,[1] Lyora A. Cohen,[1] Shirly Belizowsky-Moshe,[1] Lena Lifshitz,[1] Jing Ma,[2] Wei Li,[2] Ellina Kesselman,[3] Inbal Abutbul-Ionita,[3] Dganit Danino,[3] Lucia Gutierrez,[4] Huihui Li,[5] Kuanyu Li,[5] Huifang Lou,[6] Maria Regoni,[7] Maura Poli,[7] Fabian Glaser,[8] Tracey A. Rouault,[9] and Esther G. Meyron-Holtz[1]

[1]Laboratory for Molecular Nutrition, Faculty of Biotechnology and Food Engineering, Technion, Technion City, Haifa, Israel;
[2]Center for Medical Genetics, Beijing Children's Hospital, Capital Medical University, Beijing Pediatric Research Institute, MOE Key Laboratory of Major Diseases in Children, Beijing, China;
[3]CryoEM Laboratory of Soft Matter, Faculty of Biotechnology and Food Engineering, Technion, Technion City, Haifa, Israel;
[4]Departamento de Química Analítica, Instituto de Nanociencia de Aragón, Universidad de Zaragoza, Zaragoza, Spain;
[5]Medical School of Nanjing University, Nanjing, China;
[6]Department of Neurobiology, Zhejiang University School of Medicine, Hangzhou, China;
[7]Department of Molecular and Translational Medicine, Università degli Studi di Brescia, Brescia, Italy;
[8]The Lorry I. Lokey Interdisciplinary Center for Life Sciences and Engineering, Technion, Technion City, Haifa, Israel; and
[9]Molecular Medicine Program, Eunice Kennedy Shriver National Institute of Child Health and Human Development, National Institutes of Health, Bethesda, MD
Corresponding author.

Received 2017 Feb 17; Accepted 2017 Oct 18.

Key Points

- Iron-loaded ferritin is secreted via both the nonclassical secretory autophagy and multivesicular body–exosome pathways.
- A motif on both ferritin subunits is involved in the regulation of ferritin secretion.

Abstract

Ferritin turnover plays a major role in tissue iron homeostasis, and ferritin malfunction is associated with impaired iron homeostasis and neurodegenerative diseases. In most eukaryotes, ferritin is considered an intracellular protein that stores iron in a nontoxic and bioavailable form. In insects, ferritin is a classically secreted protein and plays a major role in systemic iron distribution. Mammalian ferritin lacks the signal peptide for classical endoplasmic reticulum–Golgi secretion but is found in serum and is secreted via a nonclassical lysosomal secretion pathway. This study applied bioinformatics and biochemical tools, alongside a protein trafficking mouse models, to characterize the mechanisms of ferritin secretion. Ferritin

trafficking via the classical secretion pathway was ruled out, and a 2:1 distribution of intracellular ferritin between membrane-bound compartments and the cytosol was observed, suggesting a role for ferritin in the vesicular compartments of the cell. Focusing on nonclassical secretion, we analyzed mouse models of impaired endolysosomal trafficking and found that ferritin secretion was decreased by a BLOC-1 mutation but increased by BLOC-2, BLOC-3, and Rab27A mutations of the cellular trafficking machinery, suggesting multiple export routes. A 13-amino-acid motif unique to ferritins that lack the secretion signal peptide was identified on the BC-loop of both subunits and plays a role in the regulation of ferritin secretion. Finally, we provide evidence that secretion of iron-rich ferritin was mediated via the multivesicular body–exosome pathway. These results enhance our understanding of the mechanism of ferritin secretion, which is an important piece in the puzzle of tissue iron homeostasis.

Visual Abstract

Introduction

Iron plays a central role in many metabolic pathways, such as oxygen transport, energy production, and erythropoiesis, which require strict regulation to avoid the toxic effects of excess iron.[1,2] In mammals, the amount of dietary iron absorbed and lost daily is small compared with the amount of iron recycled internally, and iron recycling is achieved by regulating cellular iron uptake and release.[3] The dominant iron-uptake system varies between cells and can involve the transferrin–transferrin receptor system, erythrophagocytosis, divalent metal transporter 1, or other systems.[4] Iron is predominantly released from cells by ferroportin, a ferrous iron transporter,[5,6] but heme export and ferritin secretion are alternative routes for cellular iron release.[7,8]

In mammals, ferritin is an iron-storage protein that stores ∼2000 ferric iron atoms in a soluble and nontoxic but bioavailable form.[9-11] Ferritin is composed of 2 subunits, H and L, that assemble to a 24-subunit multimer.[12] The H subunit bears ferroxidase activity, which converts Fe^{2+} to Fe^{3+} during iron entry into the ferritin shell, whereas the L subunit facilitates nucleation of the iron core.[13] Ferritin synthesis and degradation are both controlled by cellular iron status; when iron levels are low, ferritin synthesis is low because of translational repression.[14] Ferritin entry into lysosomes for degradation, mediated by the selective autophagy receptor NCOA4, is elevated when the cell is in need of iron for cellular usage. Conversely, when iron levels are high, ferritin entry to the lysosome is decreased.[15,16] It is generally accepted that ferritin is predominantly cytosolic,[10,17,18] but ferritin also demonstrates punctate distribution[8,19-22] and has been associated with vesicular location.[23,24]

Small amounts of ferritin are found in serum and other extracellular fluids, with macrophages being the main cellular source of serum ferritin in mice.[8,25-27] Serum ferritin levels serve in the differential diagnosis of anemia and as an indicator for numerous conditions, including inflammatory, neurodegenerative, and malignant diseases.[28-30] However, little is known about the mechanisms underlying ferritin intracellular trafficking and secretion. Most secreted proteins in eukaryotes use the classical endoplasmic reticulum (ER)–Golgi secretion pathway and are characterized by a signal peptide (SP), which is a leader sequence that mediates protein entry to the ER.[31,32] Despite the absence of a leader sequence, it was suggested that ferritin is secreted through the ER–Golgi route.[33] However, we showed evidence that ferritin is secreted through the nonclassical lysosomal pathway, specifically through secretory lysosomes.[8] Ferritin may enter the lysosome via NCOA4. However, NCOA4 is elevated when cellular iron is low, whereas serum ferritin is elevated when systemic iron is high.[34,35] In addition,

knockdown of NCOA4 increases ferritin secretion from monocytic cells, implying that other secretion routes may be involved. Furthermore, secretion through a NCOA4-independent "secretory autophagy" pathway was described for ferritin and interleukin 1β.[36]

Vesicle trafficking to specialized lysosome-related organelles (LROs) is regulated in mice by at least 15 genes. Mutants in these genes serve as models for the inherited Hermansky-Pudlak syndrome (HPS), which is caused by abnormalities in the synthesis and/or trafficking of LROs, such as melanosomes. *HPS* genes control a wide range of physiological processes including pigmentation, lysosome secretion and neuronal functions. Most of the HPS proteins are components of 3 multisubunit complexes named biogenesis of lysosome-related organelles complexes (BLOCs), which orchestrate the biogenesis and trafficking of LROs.[37-39] Vesicle trafficking is also regulated by Rab GTPases such as Rab27A.[40] Mutation in the *RAB27A* gene results in Griscelli syndrome, an autosomal disorder characterized by hypopigmentation and immunodeficiency.[41,42] BLOC-1 functions at an early stage of endolysosomal trafficking,[43] whereas BLOC-2, BLOC-3, and Rab27a are involved at later stages.[43,44]

Monoubiquitination was shown on ferritin,[45] suggesting that the multivesicular body (MVB)–exosome pathway may be relevant for ferritin secretion as well. Furthermore, ferritin was detected in urinary exosomes as part of proteomic screen.[46,47] MVBs are generated by invagination of endosomal membranes into large cisternae, creating intraendosomal vesicles. MVBs then fuse with either lysosomes or the cell membrane, followed by their release as "exosomes" into the extracellular space.[48,49]

In the current work, we describe novel pathways for ferritin secretion from mouse macrophages. We show that intracellular ferritin does not colocalize with Golgi apparatus and early endosome markers and that ferritin expression and secretion are not affected by an agent that disrupts the Golgi structure. Ferritin was located in punctate structures that expressed markers of the late endolysosomal compartment; cellular fractionation demonstrated the distribution of ferritin between the cytosolic and lysosomal fractions. The role of the endolysosomal pathway in ferritin secretion was further characterized using mice with impaired endolysosomal trafficking in which serum ferritin levels were greatly affected. Finally, we identify a unique motif that is important for nonclassical secretory pathways and provide evidence that ferritin-bound iron is secreted through exosomes.

Methods

Cell cultures and DNA transfections

Primary bone marrow–derived macrophages (BMDMs) were isolated and cultured as previously described.[50] RAW264.7 cells were grown in Dulbecco's modified Eagle medium (Sigma-Aldrich, Rehovot, Israel) supplemented with 10% heat-inactivated fetal bovine serum, 2 mM L-glutamine, 100 U/mL penicillin, and 100 μg/mL streptomycin (Biological Industries, Beit-Haemek, Israel). When indicated, cells were treated with 100 μg/mL ferric ammonium citrate (FAC) for 24 hours to increase cellular ferritin content. Transfection of the GFP-NCOA4 construct (a kind gift from Alec Kimmelman, Harvard Medical School, Boston, MA) was carried out using the Lipofectamine 2000 reagent (Invitrogen, Carlsbad, CA), according to the manufacturer's instructions. For transfection of the ferritin constructs, CalFectin (SignaGen Laboratories, Rockville, MD) was used.

Immunofluorescence and iron stain

Immunofluorescence staining was performed as previously described.[8,19] Iron staining of gels was performed using the Perls-DAB stain, as previously described.[19]

Subcellular fractionation and immunoblotting

Differential detergent fractionation, to obtain a fraction enriched for membrane-defined vesicles in general, and subcellular fractionation, to obtain lysosome-enriched fractions, were performed as previously described.[51,52] Fractions were lysed and subjected to sodium dodecyl sulfate polyacrylamide gel electrophoresis (SDS-PAGE) and immunoblot with the indicated antibodies.

Isolation of exosomes by ultracentrifugation, sample preparation for TEM, and analysis

Exosomes were isolated from cell culture medium, as previously described.[53] Ferritin cores were determined by transmission electron microscopy (TEM) using a JEOL (JEM-2100) electron microscope. Negative-stain TEM and cryo-TEM experiments were performed using a Tecnai T12 G2 TEM, and images were digitally captured using a Gatan Ultrascan 1000 camera. Cryo-TEM vitrified samples were examined using imaging procedures as previously described.[54]

Animal studies

All mice were on a C57BL/6J background, except for Rab27A$^{-/-}$ mice, which were on a C3H background. All mouse experiments were performed under ethics committee approval for animal experiments (granted to E.G.M.-H., W.L., and H. Lou, ethics numbers IL-042-03-11 and IL-091-08-15, Technion; KYD-2006-002, IGDB). A detailed description of mouse mutations and phenotypes is provided in supplemental Methods (available on the *Blood* Web site). Blood samples were tested by a routine veterinary laboratory in a blinded manner for complete blood count, iron, and inflammatory markers.

Additional methods

All other methods, including enzyme-linked immunosorbent assay, metabolic labeling and pulse-chase analysis, ferrozine iron assay, computational tools, and targeted deletion of human ferritin H and L subunits by clustered regularly interspaced short palindromic repeats/Cas9 and murine ferritin H-subunit mutagenesis, are described in supplemental Methods.

Results

Intracellular ferritin is found in membrane-bound vesicle-fractions, specifically in the late endolysosomal compartment

To further characterize ferritin secretory pathways, we visualized ferritin subcellular distribution in murine BMDMs in the presence of iron (100 μg/mL FAC). A punctate distribution of intracellular ferritin was observed (Figure 1), in accordance with multiple images published previously.[8,19-22] When testing for ferritin colocalization with several major organelle markers, we found that ferritin colocalized with a late endolysosomal marker (Figure 1C), but not with *cis*-Golgi and early endosome markers (Figure 1A-B). We also observed that ferritin partially colocalized with NCOA4 (supplemental Figure 1), a cargo receptor mediating ferritinophagy.[55] These results suggest that ferritin is found in vesicular compartments of the cell in iron-replete conditions.

Two subcellular fractionation approaches were employed to further characterize vesicular ferritin. Ferritin was found located in both the cytosolic and membrane-bound fractions (Figure 2A). Normalization and quantification of the subcellular distribution showed twofold more ferritin in the membrane-bound vesicle fraction compared with the cytosol, and the S-subunit, which was previously observed,[8,56] was found predominantly in the membrane fraction (Figure 2B). When specifically isolating a lysosome-enriched fraction, the S/L-ferritin subunit ratio was ∼11-fold ($P < .01$) and 7-fold ($P < .05$) higher in the lysosomal

fraction than in whole-cell lysate, with and without the addition of iron, respectively (Figure 2D). Using electron microscopy, we also found that ferritin in all fractions contained iron (Figure 2E, confirmed by energy-dispersive spectroscopy analysis; supplemental Figure 2).

Ferritin is secreted through nonclassical pathways

To further study the role of the endolysosomal trafficking machinery in ferritin secretion, we examined mice with defects in this pathway. We used serum ferritin levels in these mice as an indicator for ferritin secretion and found large differences. Three genotypes showed different degrees of elevated serum ferritin concentrations compared with wild-type (WT) mice, while BLOC-1$^{-/-}$ mice showed a threefold decrease in serum ferritin levels (Figure 3A). Serum iron and transferrin saturation were normal in all mice (Figure 3B-C). Inflammation markers were also normal (supplemental Figure 3). Liver iron showed an approximately twofold increase in BLOC-1$^{-/-}$, BLOC-2$^{-/-}$, and Rab27A$^{-/-}$ and was unchanged in BLOC-3$^{-/-}$ mice compared with WT mice (Figure 3D), indicating that there is no correlation between serum ferritin levels and liver iron in these mice. Moreover, liver transferrin receptor levels were unchanged in all mice (Figure 3E). Thus, the serum ferritin changes in these mice were not caused by systemic iron fluctuations or inflammation, strengthening the notion that defects in endolysosomal trafficking machinery impact the levels of secreted ferritin.

Although ferritin did not colocalize with the Golgi apparatus (Figure 1A), we tested whether ferritin is secreted through the classical ER–Golgi pathway. To this end, brefeldin A (BFA), an agent that disrupts the Golgi structure (Figure 4B),[57] was administered to murine BMDMs, and the medium was later subjected to a pulse chase analysis (Figure 4A). BFA did not induce accumulation of intracellular ferritin and did not inhibit ferritin secretion over time, thereby excluding the classical ER–Golgi route as a pathway for ferritin secretion.

To better understand the evolution of the classical and nonclassical pathways for ferritin secretion, we used phyloT[58] and Dendroscope[59] bioinformatics tools to create a phylogenetic tree of ferritins from eukaryotic organisms containing or lacking the classical ER targeting sequence (Figure 5A, based on sequences listed in supplemental Figure 8).[60] The unique pattern received in the phylogenetic tree reinforced the previously known distribution of SP in ferritin. Specifically, classical SP sequences were found in many insects but absent in most other eukaryotes, including mammals (Figure 5A, red and black, respectively; supplemental Figure 7).[61] We reasoned that the ferritins that lack the SP may contain a sequence needed for nonclassical pathways and thus looked for motifs that are unique to these ferritins. A 13-amino-acid motif (residues 74-86 on the mouse H subunit and residues 70 to 82 on the mouse L subunit) that was highly enriched (94%) in the SP-negative group and less enriched (48%) in the SP-positive group was identified (Figure 5B; supplemental Figure 4, motif 4). The motif was further visualized on the mouse H-chain ferritin crystal structure (Protein Data Bank: 3wnw) and located on an unstructured elongated loop between the B and C helices termed the BC-loop.[62] The motif is oriented almost entirely toward the interface between 2 neighboring ferritin subunits, thus forming a continuum zipper-like structure (Figure 5C) that functions as a dimerization motif. Application of optimal docking area (ODA)[63] software to compute the probabilities of amino acid engagement in protein–protein interactions predicted that most motif residues participate in putative protein–protein interactions (Figure 5D-F; amino acids with high probability of interaction are shown in red). Strikingly, R79, F81, and Q83 of the motif are exposed to the surface of the assembled 24-mer (Figure 5F-G) and thus are excellent candidates for interaction with other proteins. Thus, site-directed mutagenesis efforts focused on these 3 residues. To this end, ferritin secretion from human ferritin H- and L-subunit–knockout HeLa cells transfected with plasmid encoding the WT murine H subunit (FTH^{WT}) or plasmids containing a point mutation in R79, F81, or Q83 was analyzed. FTH^{F81A} and FTH^{Q83A} caused

marked increase in ferritin secretion and thus demonstrated an inhibitory role in ferritin secretion (Figure 5H). Both mutations did not impact basic ferritin functions, such as protein assembly to a 24-mer or iron incorporation (supplemental Figure 5).

These data suggest that ferritin is secreted via the endolysosomal system, where ferritin can take more than one exit route from this system. Due to the reported monoubiquitination and appearance in urinary exosomes of ferritin,[45-47] we examined the MVB–exosome pathway. Both ferritin and the exosomal marker TSG101 were detected in exosomes purified from the medium of RAW264.7 macrophages (Figure 6A). Negative staining (TEM) demonstrated the typical cup-shaped morphology of these nanovesicles, which were ∼100 nm in size[48,49] (Figure 6B). However, because the exosome isolation protocol includes ultracentrifugation steps, free ferritin released through the secretory-autophagy route may coprecipitate with exosomes because of its heavy iron cores (Figure 6B; supplemental Figure 6, red circles). Thus, we further analyzed these TSG-101–positive exosomal fractions by cryo-TEM without any staining and found typical ferritin-iron cores within exosomal structures (Figure 6C, white arrows). Size analysis of ∼100 iron cores demonstrated an average core size of 3.8 ± 0.9 nm and 4.9 ± 0.8 nm inside and outside the exosomes, respectively ($P < .0001$). Taken together, we propose that mouse ferritin is secreted not only by the nonclassical secretory-autophagy route but also through the MVB–exosome pathway.

Discussion

Intracellular ferritin trafficking

Ferritin is the major intracellular iron-storage protein in many organisms.[10,62,64] Although it has been generally accepted that ferritin is predominantly cytosolic,[10,17,18] it also displays punctate, uneven distribution[8,19-22] that has been associated with vesicular location.[23,24] Ferritin's entrance into the endolysosomal system has been shown to be dependent on the autophagy receptor NCOA4, and recently, the specialized secretory-autophagy receptor TRIM16 was ascribed a role in ferritin entry to secretory autophagosomes.[36] Focusing on macrophage cell models, we found ferritin in the endolysosomal system, but not the Golgi apparatus (Figure 1A). The classical ER–Golgi inhibitor BFA did not affect cellular ferritin localization (Figure 4B) or secretion (Figure 4A), which strongly implied, in contrast to the general consensus, that ferritin does not traffic through the classical ER–Golgi secretion pathway.[33] Further, most ferritin colocalized with a late-endolysosomal marker, supporting the notion that iron-loaded ferritin is trafficked and secreted via a nonclassical vesicular route. However, some punctate ferritin entities did not colocalize with this marker (Figure 1D, red arrows), suggesting the presence of membrane-bound fractions of ferritin that are not lysosomal.

Bioinformatics of ferritin secretion

In insects, ferritin is secreted via the classical ER–Golgi route and contains an ER-targeting SP.[61] Analysis of the distribution of eukaryotic ferritins on a taxonomy-based phylogenetic tree (Figure 5A; supplemental Figure 7) showed that most of the tested eukaryotic organisms do not have a classical SP on their ferritins. We identified a motif with a high likelihood of engaging in protein–protein interactions that was highly enriched in all ferritins lacking the SP but appeared in only 48% of classically secreted ferritins (Figures 5B; supplemental Figure 4, motif 4). This suggested that classically secreted ferritins had no need to conserve this motif, indicating that it may serve a function in the nonclassical secretion pathway. Furthermore, the amino acids colored red in Figure 5D-F are mostly exposed to the solvent and very likely to participate in protein–protein interaction (Figure 5F). Although most amino acids in this patch likely interact with neighboring ferritin subunits, R22 (Figure 5G, orange) interacts with NCOA4 and is the key

arginine required for delivery of ferritin to degrading lysosomes.[16] Mutation of residues F81 and Q83 led to highly increased ferritin secretion (Figure 5H), suggesting they have an inhibitory role in ferritin secretion, presumably by preventing ferritin from entering the secretion route.

Analysis of serum ferritin in mice with endolysosomal trafficking defects suggests 2 alternative nonclassical routes for ferritin secretion

We previously proposed that serum ferritin, which is the most accessible secreted ferritin in a whole organism, is an actively secreted ferritin containing L and H subunits and iron, although its iron content and H/L-subunit ratio are much lower than in any known intracellular ferritin. In contrast, ferritin secreted from cell lines or primary BMDMs is similar to intracellular ferritin in its iron content and subunit composition, suggesting that cytosolic ferritin enters a secretory pathway and is secreted without much processing. Although the discrepancy between secreted ferritin and serum ferritin is not well understood, serum ferritin levels are in good correlation with macrophage iron loading[8] (Figure 4A). To further understand the reported pathway of secretory autophagy described for interleukin-1β and ferritin,[8,36] we focused on mice with defects in trafficking via LROs (secretory lysosomes or secretory autophagy). Serum ferritin levels were significantly reduced in BLOC-1–deficient mice but significantly elevated in BLOC-2–, BLOC-3–, and Rab27A-deficient mice (Figure 3A), suggesting that specific defects in early or later stages of vesicle trafficking to LROs have opposite effects on ferritin secretion. Studies have shown intracellular accumulation of prelysosomes in the cortical neurons of the BLOC-1–component snapin-knockout mice[65] and endolysosomes of mouse embryonic fibroblasts from 3 different BLOC-1 subunit–null mice (BLOS1-KO, BLOS2-KO, or pallid).[66,67] Thus, ferritin may be trapped in these prelysosomes or endolysosomes and targeted for degradation in BLOC-1–deficient mice. In contrast, in BLOC-2–, BLOC-3–, or Rab27A-deficient mice, lysosomal function or secretion was blocked, causing ferritin to accumulate and exit the cell through the alternative MVB route via exosomes. This notion is supported by the fact that the number of MVBs was increased, whereas fewer lysosomes were observed in BLOC-2–deficient cells.[68] Interestingly, the size of MVBs was also strongly increased by Rab27A silencing.[69] Although ferritin enters the protein-degrading compartment of the endolysosomal system through the autophagy receptor NCOA4, a recent study suggested that NCOA4 does not take part in ferritin secretion.[36] NCOA4-null mice showed elevated serum-ferritin levels, further demonstrating that ferritin secretion increases when ferritin accumulates because of decreased degradation. Finally, BLOC-1–deficient mice exhibited impaired MVB maturation,[70] which further explains the lower ferritin secretion in these mice. Taken together, these observations suggest that ferritin is secreted via 2 nonclassical routes.

Ferritin secretion through the MVB–exosome pathway

Exosomes are secreted upon fusion of MVBs with the plasma membrane. Exosomes in body fluids play an important role in exchanging information between cells and can act in a paracrine or even endocrine manner to modify gene expression, signaling, and overall functioning of adjacent or distant cells.[71] Recently, it was reported that the iron-carrier molecules transferrin and lactoferrin are found in exosomes and can be delivered into mammalian cells via this route.[72] Ferritin was also found in human urinary exosomes in a large-scale proteomic analysis.[46,47] However, neither local ferritin secretion via exosomes nor its iron content have been reported. Here, we present evidence that ferritin-bound iron is secreted via exosomes (Figure 6). This ability of exosomes to transfer iron-carrier molecules between cells may play an important role in intercellular communication and the maintenance of iron homeostasis under physiological conditions.

Possible functions of secreted ferritin

Ferroportin is the only known ferrous iron exporter. However, we and others suggested that secreted ferritin may function as an iron exporter of ferric iron[8,19,73]; experimental evidence was provided by both Leimberg et al[74] and Sibille et al,[75] who showed that ferritin secreted by hepatocytes and macrophages functioned as an iron-donor protein. This suggests that ferritin secreted by macrophages, which specialize in iron acquisition, can be taken up by cell types specialized in iron storage, such as hepatocytes, or high-iron consumers, such as developing erythroid cells. The existence of ferritin receptors such as murine TIM2, human TfR1, and SCARA5 on these cells[76-78] strengthens our hypothesis, whereas exosome-mediated ferritin transport is independent of receptor-mediated ferritin uptake. However, there remains a missing link between the secreted ferritin that is iron bound and bears the subunit composition of its intracellular counterpart and the serum ferritin that contains very little iron and H subunits only. We believe that ferritins containing iron and at least 1 H subunit are locally delivered to cells via vesicular structures, such as exosomes, and via receptor-mediated internalization and thus never reach the serum. Only iron-poor L-subunit ferritins, which are barely taken up by the H-specific ferritin receptors, reach the serum. Vesicular location and secretion of ferritin was also found in additional cell types, such as Sertoli cells[19] and HepG2 and Caco-2 epithelial cells (S.B.-M., unpublished data), and thus, the described machineries for regulated ferritin secretion may not be unique to macrophages. It will be interesting to further investigate the ferritin-secretion pathways in both hepatocytes and epithelial barrier cells. Lastly, because many of the major neurodegenerative diseases are associated with iron and ferritin misdistribution in the brain, defects in ferritin trafficking and secretion may play a central role in the development of these diseases. Taken together, our findings and evidence that exosomes pass the blood–brain barrier[79] may also shed light on iron entry to the adult brain and neurodegenerative diseases accompanied by impaired iron distribution in the brain.

Supplementary Material

The online version of this article contains a data supplement.

Acknowledgments

The authors thank A. M. Konijn (Hebrew University, Jerusalem, Israel) for introducing us to ferritin and sharing all his antibodies, Theodore Iancu (Technion, Haifa, Israel) for avid discussion until his recent death, Alec Kimmelman (Harvard Medical School, Boston, MA) for the NCOA4-GFP-construct, and Yehudit Posen for rigorous editing of the manuscript. The authors also thank the LS&E Infrastructure Center at the Technion, Nitsan Dahan, Anna Parnis, Shirley Larom, Faris Salama, Nitsan Fourier, Mamdoh Khateb, Yael Danin-Poleg, and Inbar Freilich for assistance; Liron Abrahami and Tomer Levy for bioinformatics work; and Leon Rosentsvit, Lulu Fahoum, Yael Haimovich, Michella Asperti, Yael Leichtmann-Bardoogo, and Sofia Belikovetsky for continued support and inspiration.

L.G. acknowledges financial support from the Ramón y Cajal subprogram (RYC-2014-15512). This research was supported by The Israel Science Foundation (grant 1444/13 to E.G.M.-H.), the US–Israel Binational Science Foundation (grant 2007466 to E.G.M.-H. and T.A.R.), and the National Science Foundation of China (grants 91539204 and 31230046 to W.L.).

Footnotes

The publication costs of this article were defrayed in part by page charge payment. Therefore, and solely to indicate this fact, this article is hereby marked “advertisement” in accordance with 18 USC section 1734.

Authorship

Contribution: M.T.-R., L.A.C., S.B.-M., L.L., T.A.R., and E.G.M.-H. designed the research; M.T.-R., L.S., and E.G.M.-H. designed and performed in vitro experiments; M.T.-R., J.M., W.L., H. Li, K.L., H. Lou, and E.G.M.-H. designed and performed in vivo and all BLOCs- and Rab27A-related analyses; M.T.-R., L.G., E.K., I.A.-I., D.D., and E.G.M.-H. designed and performed electron microscopy experiments; M.T.-R., D.B., L.S., F.G., and E.G.M.-H. designed and performed bioinformatics; M.R. and M.P. designed and produced HeLa FTH-FTL–knockout cells by clustered regularly interspaced short palindromic repeats/Cas9; and M.T.-R., T.A.R., and E.G.M.-H. wrote and edited the manuscript.

Conflict-of-interest disclosure: The authors declare no competing financial interests.

Correspondence: Esther G. Meyron-Holtz, Laboratory for Molecular Nutrition, Faculty of Biotechnology and Food Engineering, Technion, Technion City, Haifa 32000, Israel; e-mail: meyron@tx.technion.ac.il.

References

1. Anderson GJ, Vulpe CD. Mammalian iron transport. *Cell Mol Life Sci*. 2009;66(20):3241-3261. [PubMed: 19484405]

2. Outten FW, Theil EC. Iron-based redox switches in biology. *Antioxid Redox Signal*. 2009;11(5):1029-1046. [PMCID: PMC2842161] [PubMed: 19021503]

3. Anderson GJ. Ironing out disease: inherited disorders of iron homeostasis. *IUBMB Life*. 2001;51(1):11-17. [PubMed: 11419690]

4. Frazer DM, Anderson GJ. The regulation of iron transport. *Biofactors*. 2014;40(2):206-214. [PubMed: 24132807]

5. Knutson M, Wessling-Resnick M. Iron metabolism in the reticuloendothelial system. *Crit Rev Biochem Mol Biol*. 2003;38(1):61-88. [PubMed: 12641343]

6. Mikhael M, Sheftel AD, Ponka P. Ferritin does not donate its iron for haem synthesis in macrophages. *Biochem J*. 2010;429(3):463-471. [PubMed: 20515444]

7. Ponka P, Sheftel AD, English AM, Scott Bohle D, Garcia-Santos D. Do mammalian cells really need to export and import heme? *Trends Biochem Sci*. 2017;42(5):395-406. [PubMed: 28254242]

8. Cohen LA, Gutierrez L, Weiss A, et al. . Serum ferritin is derived primarily from macrophages through a nonclassical secretory pathway. *Blood*. 2010;116(9):1574-1584. [PubMed: 20472835]

9. Ford GC, Harrison PM, Rice DW, et al. . Ferritin: design and formation of an iron-storage molecule. *Philos Trans R Soc Lond B Biol Sci*. 1984;304(1121):551-565. [PubMed: 6142491]

10. Harrison PM, Arosio P. The ferritins: molecular properties, iron storage function and cellular regulation. *Biochim Biophys Acta*. 1996;1275(3):161-203. [PubMed: 8695634]

11. Koorts AM, Viljoen M. Ferritin and ferritin isoforms I: structure-function relationships, synthesis, degradation and secretion. *Arch Physiol Biochem*. 2007;113(1):30-54. [PubMed: 17522983]

12. Arosio P, Ingrassia R, Cavadini P. Ferritins: a family of molecules for iron storage, antioxidation and more. *Biochim Biophys Acta* 2009;1790:589-599. [PubMed: 18929623]

13. Santambrogio P, Levi S, Cozzi A, Corsi B, Arosio P. Evidence that the specificity of iron incorporation into homopolymers of human ferritin L- and H-chains is conferred by the nucleation and ferroxidase centres. *Biochem J*. 1996;314(Pt 1):139-144. [PMCID: PMC1217016] [PubMed: 8660274]

14. Rouault TA, Tang CK, Kaptain S, et al. . Cloning of the cDNA encoding an RNA regulatory protein--the human iron-responsive element-binding protein. *Proc Natl Acad Sci USA*. 1990;87(20):7958-7962. [PMCID: PMC54871] [PubMed: 2172968]

15. Rouault TA. The role of iron regulatory proteins in mammalian iron homeostasis and disease. *Nat Chem Biol*. 2006;2(8):406-414. [PubMed: 16850017]

16. Mancias JD, Pontano Vaites L, Nissim S, et al. . Ferritinophagy via NCOA4 is required for erythropoiesis and is regulated by iron dependent HERC2-mediated proteolysis. *eLife*. 2015;4:4. [PMCID: PMC4592949] [PubMed: 26436293]

17. Speyer BE, Fielding J. Ferritin as a cytosol iron transport intermediate in human reticulocytes. *Br J Haematol*. 1979;42(2):255-267. [PubMed: 465371]

18. Arosio P, Elia L, Poli M. Ferritin, cellular iron storage and regulation. *IUBMB Life*. 2017;69(6):414-422. [PubMed: 28349628]

19. Leichtmann-Bardoogo Y, Cohen LA, Weiss A, et al. . Compartmentalization and regulation of iron metabolism proteins protect male germ cells from iron overload. *Am J Physiol Endocrinol Metab*. 2012;302(12):E1519-E1530. [PubMed: 22496346]

20. Meyron-Holtz EG, Cohen LA, Fahoum L, et al. . Ferritin polarization and iron transport across monolayer epithelial barriers in mammals. *Front Pharmacol*. 2014;5:194. [PMCID: PMC4142484] [PubMed: 25202274]

21. Rouault TA, Zhang D-L, Jeong SY. Brain iron homeostasis, the choroid plexus, and localization of iron transport proteins. *Metab Brain Dis*. 2009;24(4):673-684. [PMCID: PMC2788140] [PubMed: 19851851]

22. Vanoaica L, Darshan D, Richman L, Schümann K, Kühn LC. Intestinal ferritin H is required for an accurate control of iron absorption. *Cell Metab*. 2010;12(3):273-282. [PubMed: 20816093]

23. Van Deurs B, Von Bülow F, Møller M. Vesicular transport of cationized ferritin by the epithelium of the rat choroid plexus. *J Cell Biol*. 1981;89(1):131-139. [PMCID: PMC2111774] [PubMed: 7228898]

24. Clough G, Michel CC. The role of vesicles in the transport of ferritin through frog endothelium. *J Physiol*. 1981;315(1):127-142. [PMCID: PMC1249372] [PubMed: 6975816]

25. Worwood M. Serum ferritin. *CRC Crit Rev Clin Lab Sci*. 1979;10(2):171-204. [PubMed: 378539]

26. Blake DR, Bacon PA, Eastham EJ, Brigham K. Synovial fluid ferritin in rheumatoid arthritis. *BMJ*. 1980;281(6242):715-716. [PMCID: PMC1713960] [PubMed: 7427414]

27. Sindic CJ, Collet-Cassart D, Cambiaso CL, Masson PL, Laterre EC. The clinical relevance of ferritin concentration in the cerebrospinal fluid. *J Neurol Neurosurg Psychiatry*. 1981;44(4):329-333. [PMCID: PMC490956] [PubMed: 7241160]

28. Knovich MA, Storey JA, Coffman LG, Torti SV, Torti FM. Ferritin for the clinician. *Blood Rev*. 2009;23(3):95-104. [PMCID: PMC2717717] [PubMed: 18835072]

29. Rosário C, Zandman-Goddard G, Meyron-Holtz EG, D'Cruz DP, Shoenfeld Y. The hyperferritinemic syndrome: macrophage activation syndrome, Still's disease, septic shock and catastrophic antiphospholipid syndrome. *BMC Med*. 2013;11(1):185. [PMCID: PMC3751883] [PubMed: 23968282]

30. Lipschitz DA, Cook JD, Finch CA. A clinical evaluation of serum ferritin as an index of iron stores. *N Engl J Med*. 1974;290(22):1213-1216. [PubMed: 4825851]

31. Nickel W, Rabouille C. Mechanisms of regulated unconventional protein secretion. *Nat Rev Mol Cell Biol*. 2009;10(2):148-155. [PubMed: 19122676]

32. Voorhees RM, Hegde RS. Toward a structural understanding of co-translational protein translocation. *Curr Opin Cell Biol*. 2016;41:91-99. [PubMed: 27155805]

33. Ghosh S, Hevi S, Chuck SL. Regulated secretion of glycosylated human ferritin from hepatocytes. *Blood*. 2004;103(6):2369-2376. [PubMed: 14615366]

34. Worwood M. The diagnostic value of serum ferritin determinations for assessing iron status. *Haematologia (Budap)*. 1987;20(4):229-235. [PubMed: 3322966]

35. Torti SV, Torti FM. Iron and ferritin in inflammation and cancer. *Adv Inorg Biochem*. 1994;10:119-137. [PubMed: 8203285]

36. Kimura T, Jia J, Kumar S, et al. . Dedicated SNAREs and specialized TRIM cargo receptors mediate secretory autophagy. *EMBO J*. 2017;36(1):42-60. [PMCID: PMC5210154] [PubMed: 27932448]

37. Dell'Angelica EC. The building BLOC(k)s of lysosomes and related organelles. *Curr Opin Cell Biol*. 2004;16(4):458-464. [PubMed: 15261680]

38. Wei A-H, Li W. Hermansky-Pudlak syndrome: pigmentary and non-pigmentary defects and their pathogenesis. *Pigment Cell Melanoma Res*. 2013;26(2):176-192. [PubMed: 23171219]

39. Gautam R, Novak EK, Tan J, Wakamatsu K, Ito S, Swank RT. Interaction of Hermansky-Pudlak syndrome genes in the regulation of lysosome-related organelles. *Traffic*. 2006;7(7):779-792. [PubMed: 16787394]

40. Tolmachova T, Anders R, Stinchcombe J, et al. . A general role for Rab27a in secretory cells. *Mol Biol Cell*. 2004;15(1):332-344. [PMCID: PMC307551] [PubMed: 14617806]

41. Ménasché G, Pastural E, Feldmann J, et al. . Mutations in RAB27A cause Griscelli syndrome associated with haemophagocytic syndrome. *Nat Genet*. 2000;25(2):173-176. [PubMed: 10835631]

42. Bahadoran P, Aberdam E, Mantoux F, et al. . Rab27a: a key to melanosome transport in human melanocytes. *J Cell Biol*. 2001;152(4):843-850. [PMCID: PMC2195788] [PubMed: 11266474]

43. Langemeyer L, Ungermann C. BORC and BLOC-1: shared subunits in trafficking complexes. *Dev Cell*. 2015;33(2):121-122. [PubMed: 25898163]

44. Wilson SM, Yip R, Swing DA, et al. . A mutation in Rab27a causes the vesicle transport defects observed in ashen mice. *Proc Natl Acad Sci USA*. 2000;97(14):7933-7938. [PMCID: PMC16648] [PubMed: 10859366]

45. De Domenico I, Vaughn MB, Li L, et al. . Ferroportin-mediated mobilization of ferritin iron precedes ferritin degradation by the proteasome. *EMBO J*. 2006;25(22):5396-5404. [PMCID: PMC1636618] [PubMed: 17082767]

46. Gonzales PA, Pisitkun T, Hoffert JD, et al. . Large-scale proteomics and phosphoproteomics of urinary exosomes. *J Am Soc Nephrol*. 2009;20(2):363-379. [PMCID: PMC2637050] [PubMed: 19056867]

47. Principe S, Jones EE, Kim Y, et al. . In-depth proteomic analyses of exosomes isolated from expressed prostatic secretions in urine. *Proteomics*. 2013;13(10-11):1667-1671. [PMCID: PMC3773505] [PubMed: 23533145]

48. Zhang M, Schekman R. Cell biology. Unconventional secretion, unconventional solutions. *Science*. 2013;340(6132):559-561. [PubMed: 23641104]

49. Colombo M, Raposo G, Théry C. Biogenesis, secretion, and intercellular interactions of exosomes and other extracellular vesicles. *Annu Rev Cell Dev Biol*. 2014;30(1):255-289. [PubMed: 25288114]

50. Weischenfeldt J, Porse B Bone marrow-derived macrophages (BMM): isolation and applications. *CSH Protoc.* 2008;2008:pdb.prot5080. [PubMed: 21356739]

51. Tong WH, Rouault T. Distinct iron-sulfur cluster assembly complexes exist in the cytosol and mitochondria of human cells. *EMBO J*. 2000;19(21):5692-5700. [PMCID: PMC305809] [PubMed: 11060020]

52. Brix K, Lemansky P, Herzog V. Evidence for extracellularly acting cathepsins mediating thyroid hormone liberation in thyroid epithelial cells. *Endocrinology*. 1996;137(5):1963-1974. [PubMed: 8612537]

53. Théry C, Amigorena S, Raposo G, Clayton A. Isolation and characterization of exosomes from cell culture supernatants and biological fluids. *Curr Protoc Cell Biol.* 2006;Chapter 3:Unit 3.22. [PubMed: 18228490]

54. Danino D. Cryo-TEM of soft molecular assemblies. *Curr Opin Colloid Interface Sci*. 2012;17(6):316-329.

55. Mancias JD, Wang X, Gygi SP, Harper JW, Kimmelman AC. Quantitative proteomics identifies NCOA4 as the cargo receptor mediating ferritinophagy. *Nature*. 2014;509(7498):105-109. [PMCID: PMC4180099] [PubMed: 24695223]

56. Andrews SC, Treffry A, Harrison PM. Siderosomal ferritin. The missing link between ferritin and haemosiderin? *Biochem J*. 1987;245(2):439-446. [PMCID: PMC1148141] [PubMed: 3663170]

57. Helms JB, Rothman JE. Inhibition by brefeldin A of a Golgi membrane enzyme that catalyses exchange of guanine nucleotide bound to ARF. *Nature*. 1992;360(6402):352-354. [PubMed: 1448152]

58. Letunic I, Bork P. Interactive Tree Of Life (iTOL): an online tool for phylogenetic tree display and annotation. *Bioinformatics*. 2007;23(1):127-128. [PubMed: 17050570]

59. Huson DH, Scornavacca C. Dendroscope 3: an interactive tool for rooted phylogenetic trees and networks. *Syst Biol*. 2012;61(6):1061-1067. [PubMed: 22780991]

60. Bailey TL, Boden M, Buske FA, et al. . MEME SUITE: tools for motif discovery and searching. *Nucleic Acids Res.* 2009;37(Web Server issue):W202-W208. [PMCID: PMC2703892] [PubMed: 19458158]

61. Pham DQD, Winzerling JJ. Insect ferritins: typical or atypical? *Biochim Biophys Acta*. 2010;1800(8):824-833. [PMCID: PMC2893279] [PubMed: 20230873]

62. Theil EC. Ferritin: structure, gene regulation, and cellular function in animals, plants, and microorganisms. *Annu Rev Biochem*. 1987;56(1):289-315. [PubMed: 3304136]

63. Fernandez-Recio J, Totrov M, Skorodumov C, Abagyan R. Optimal docking area: a new method for predicting protein-protein interaction sites. *Proteins*. 2005;58(1):134-143. [PubMed: 15495260]

64. Worwood M. Ferritin. *Blood Rev*. 1990;4(4):259-269. [PubMed: 2076473]

65. Cai Q, Lu L, Tian J-H, Zhu YB, Qiao H, Sheng ZH. Snapin-regulated late endosomal transport is critical for efficient autophagy-lysosomal function in neurons. *Neuron*. 2010;68(1):73-86. [PMCID: PMC2953270] [PubMed: 20920792]

66. Zhang A, He X, Zhang L, Yang L, Woodman P, Li W. Biogenesis of lysosome-related organelles complex-1 subunit 1 (BLOS1) interacts with sorting nexin 2 and the endosomal sorting complex required for transport-I (ESCRT-I) component TSG101 to mediate the sorting of epidermal growth factor receptor into endosomal compartments. *J Biol Chem*. 2014;289(42):29180-29194. [PMCID: PMC4200271] [PubMed: 25183008]

67. Zhou W, He Q, Zhang C, et al. . BLOS2 negatively regulates Notch signaling during neural and hematopoietic stem and progenitor cell development. *eLife*. 2016;5:5. [PMCID: PMC5094856] [PubMed: 27719760]

68. Li K, Yang L, Zhang C, Niu Y, Li W, Liu JJ. HPS6 interacts with dynactin p150Glued to mediate retrograde trafficking and maturation of lysosomes. *J Cell Sci*. 2014;127(Pt 21):4574-4588. [PubMed: 25189619]

69. Ostrowski M, Carmo NB, Krumeich S, et al. . Rab27a and Rab27b control different steps of the exosome secretion pathway. *Nat Cell Biol.* 2010;12(1):19-30. [PubMed: 19966785]

70. John Peter AT, Lachmann J, Rana M, Bunge M, Cabrera M, Ungermann C. The BLOC-1 complex promotes endosomal maturation by recruiting the Rab5 GTPase-activating protein Msb3. *J Cell Biol*. 2013;201(1):97-111. [PMCID: PMC3613695] [PubMed: 23547030]

71. Kourembanas S. Exosomes: vehicles of intercellular signaling, biomarkers, and vectors of cell therapy. *Annu Rev Physiol*. 2015;77(1):13-27. [PubMed: 25293529]

72. Malhotra H, Sheokand N, Kumar S, et al. . Exosomes: tunable nano vehicles for macromolecular delivery of transferrin and lactoferrin to specific intracellular compartment. *J Biomed Nanotechnol*. 2016;12(5):1101-1114. [PubMed: 27305829]

73. Meyron-Holtz EG, Moshe-Belizowski S, Cohen LA A possible role for secreted ferritin in tissue iron distribution. *J Neural Transm (Vienna)* 2011;118(3):337-347. [PubMed: 21298454]

74. Leimberg JM, Konijn AM, Fibach E. Macrophages promote development of human erythroid precursors in transferrin-free culture medium. *Hematology*. 2005;10(1):73-76. [PubMed: 16019451]

75. Sibille JC, Kondo H, Aisen P. Interactions between isolated hepatocytes and Kupffer cells in iron metabolism: a possible role for ferritin as an iron carrier protein. *Hepatology*. 1988;8(2):296-301. [PubMed: 3356411]

76. Chen TT, Li L, Chung D-H, et al. . TIM-2 is expressed on B cells and in liver and kidney and is a receptor for H-ferritin endocytosis. *J Exp Med*. 2005;202(7):955-965. [PMCID: PMC2213179] [PubMed: 16203866]

77. Li JY, Paragas N, Ned RM, et al. . Scara5 is a ferritin receptor mediating non-transferrin iron delivery. *Dev Cell*. 2009;16(1):35-46. [PMCID: PMC2652503] [PubMed: 19154717]

78. Li L, Fang CJ, Ryan JC, et al. . Binding and uptake of H-ferritin are mediated by human transferrin receptor-1. *Proc Natl Acad Sci USA*. 2010;107(8):3505-3510. [PMCID: PMC2840523] [PubMed: 20133674]

79. Wood MJA, O'Loughlin AJ, Samira L. Exosomes and the blood-brain barrier: implications for neurological diseases. *Ther Deliv*. 2011;2(9):1095-1099. [PubMed: 22833906]

Figures and Tables

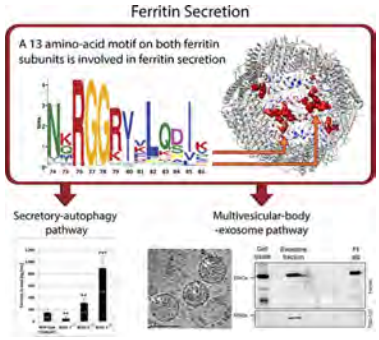
Ferritin Secretion
A 13 amino-acid motif on both ferritin subunits is involved in ferritin secretion
Secretory-autophagy pathway
Multivesicular-body -exosome pathway

Figure 1.

Ferritin colocalizes with the late endolysosomal marker cathepsin D, but not with Golgi or early endosomal markers. (A-C) Representative confocal images of ferritin (red) and subcellular compartments (green) in the Golgi apparatus (A), stained for GM-130; early endosomes (B), stained for EEA1, and late endolysosomes (C), stained for cathepsin D (CatD), in murine BMDMs grown in the presence of 100 μg/mL FAC for 24 hours. Scale bars represent 10 μm. (D) Enlargement of ferritin-CatD co-staining, with red arrows indicating ferritin, green arrows indicating late endolysosomes, and yellow arrows indicating colocalization. Negative controls were treated with secondary antibodies only and with 1 primary antibody followed by both secondary antibodies (not depicted). Sample visualization was performed with a LSM 700 (Zeiss) laser scanning inverted confocal microscope equipped with a Plan-Apochromat ×63/1.4 numerical aperture oil differential interference contrast objective.

Figure 2.

Iron-loaded ferritin is located in membrane-bound vesicles, specifically in lysosome-enriched fractions. (A) Control and iron-treated (100 μg/mL FAC for 24 hours) BMDMs were fractionated using a differential subcellular fractionation method. Total cell lysates and cytosol and membrane-bound vesicle–enriched subfractions (membranes) were separated on SDS-PAGE (40 μg protein/lane) and analyzed by western blot, with anti-L-ferritin, LAMP1 (lysosomal marker), and antitubulin (cytosolic marker) antibodies. The results of 1 out of 3 representative experiments are shown. (B) Intensity of L- and S-ferritin bands of control (Ctrl) samples were quantified using Adobe Photoshop software. Mean band intensities were normalized to whole-cell protein by volume ratios. The results of 1 out of 3 representative experiments are shown. (C) Control and iron-treated (100 μg/mL FAC for 24 hours) RAW264.7 macrophages were fractionated using a lysosomal enrichment method. Total cell lysates and lysosomal fractions were separated on SDS-PAGE and analyzed by western blot with anti-L-ferritin and anti-LAMP1 antibodies. (D) Intensity of L- and S-ferritin bands on immunoblot was quantified; each bar represents mean ± standard deviation (SD); n = 4 (*$P < .05$, **$P < .01$ compared with control samples). (E) A drop of each fraction was mounted on a carbon-coated copper grid at room temperature. Iron cores (arrows) were determined using a JEOL (JEM-2100) electron microscope operated at 200 KeV. Scale bar represents 100 nm.

Figure 3.

Serum ferritin levels are affected in mice with trafficking defects of the endolysosomal pathways. (A) Serum ferritin levels were estimated by enzyme-linked immunosorbent assay. (B) Serum iron and all other blood tests were performed by trained staff in a veterinary laboratory. (C) Transferrin saturation percentage was calculated by dividing serum iron by total iron-binding capacity and multiplying by 100. (D) Liver iron was evaluated using a colorimetric ferrozine-based assay. (E) Transferrin receptor 1 (TfR1) western blot. Liver lysates were separated by SDS-PAGE (35 µg protein/lane) and subjected to western blotting with anti-TfR1 and antiactin antibodies. Representative results in livers from 2 out of 4 mice are shown. Measurements of BLOC-1$^{-/-}$, BLOC-2$^{-/-}$, and BLOC-3$^{-/-}$ mice were compared with those of WT C57BL/6J mice. Rab27A$^{-/-}$ mice were on a C3H background and were compared with their WT counterparts. Each bar represents mean ± SD (*P < .05, **P < .01, ***P < .001). Statistical significance was evaluated by an unpaired t test using GraphPad software.

Figure 4.

Ferritin is not secreted through the classical ER–Golgi secretion pathway. (A) Murine BMDMs were metabolically labeled with ^{35}S in the presence of 100 μg/mL FAC and in presence or absence of 5 μg/mL BFA. Cells and media were collected at 0, 2, and 4 hours. Ferritin was immunoprecipitated from lysates and media with an anti-L-ferritin antibody and separated on SDS-PAGE. All samples were precleared (PC) by incubation with protein A sepharose beads alone to clear samples from nonspecific binding to the beads. L- and H-ferritin subunit band intensity was quantified using Adobe Photoshop software (each bar represents mean ± SD; n = 2). (B) Representative confocal images of ferritin (green) and the Golgi marker GM-130 (red) in murine macrophages (top, control, nontreated macrophages; bottom, BFA-treated macrophages). Negative controls were done with secondary antibodies only (insert, top panel) and with 1 primary antibody followed by both secondary antibodies to exclude channel leakage (not depicted). Scale bars represent 10 μm. Image visualization was performed on a LSM 700 (Zeiss) laser scanning inverted confocal microscope with a Plan-Apochromat ×63/1.4 numerical aperture oil differential interference contrast objective.

Figure 5.

Identification of a motif enriched in ferritins that do not have a classical secretion signal. (A) A taxonomy-based phylogenetic tree of ferritins containing or lacking the classical ER SP targeting sequence. The organisms marked red are SP positive, and the organisms marked black are SP negative. The pink area is a dominantly SP-positive cluster, and the green area is a dominantly SP-negative cluster. *Mus musculus* and *Homo sapiens* locations are marked in yellow and shown in the enlargement. (B) A 13-amino-acid motif detected by the MEME[60] and FIMO[60] tools. The motif includes residues 74 to 86 of the H subunit and residues 70 to 82 of the L subunit. (C) The motif is situated along an unstructured loop of the ferritin subunits and sits at the interface between 2 subunits (colored in cyan and gold), creating a continuous long zipper-like structure (ie, a motif dimer) with its neighbor motif. (D) R79, F81, and Q83 of the motif received high ODA scores for protein–protein interaction (high score is labeled in red and low score in blue). (E) Visualization of protein–protein interaction patch, calculated by ODA score. (F) Visualization of protein–protein interaction patches calculated by ODA score shown in the context of the whole ferritin multimer. Our motif, R22, and an additional unidentified group of residues are marked in red. (G) Motif distribution and location throughout the entire ferritin 24-mer. The motif forms a long dimer (colored in green) at the interface of 2 subunits. R79 is marked in red, and R22 is marked in orange. (H) Human ferritin H- and L-subunit–knockout HeLa cells were transfected with plasmids coding for either WT murine H-ferritin (FTH^{WT}) or FTH^{R79A}, FTH^{F81A}, or FTH^{Q83A}. Nontransfected HeLa cells (NT) were analyzed as a negative control. WT RAW264.7 (nontransfected) cells were analyzed as a positive control for both L- and H-ferritin subunits (lane 12 in “cell lysates” gel and lane 17 in “media” gel). 24 hours after transfection, cells were metabolically labeled with ^{35}S (2-hour pulse) and chased for 0, 4, and 18 hours. Cell lysates were collected after 4 and 18 hours (lanes 2-6 and 7-11 in cell lysates gel, respectively), whereas media samples were collected after 0, 4, and 18 hours (lanes 2-6, 7-11, and 12-16 in media gel, respectively). Ferritin was immunoprecipitated with an anti-murine H-ferritin antibody. All samples were precleared (PC) by incubation with protein A sepharose beads alone to clear samples from nonspecific binding to the beads. Two of these samples, 4 hours of WT cell lysates and 18 hours of WT medium, where most nonspecific binding was expected, were analyzed on the gels (lanes 1). All samples were separated by SDS-PAGE and visualized by phosphorimaging.

Figure 6.

Ferritin-iron cores are present in exosomes. (A) RAW264.7 macrophages were incubated for 24 hours in a mixture of OptiMEM I medium and Dulbecco's modified Eagle medium (1:1 volume ratio) supplemented with 10% heat-inactivated fetal bovine serum, 2 mM L-glutamine, 100 U/mL penicillin, 100 μg/mL streptomycin, 1 mg/L BSA, 20 mM β-mercaptoethanol, and 100 μg/mL FAC. To precipitate exosomes, cells were harvested, and medium was collected and centrifuged at 100 000*g* for 1.5 hours. Samples were then separated by SDS-PAGE and analyzed by western blot with anti-ferritin L-subunit and anti-TSG101 (serving as exosomal marker) antibodies. The results of 1 out of 4 experiments are shown. (B) Exosomal samples were resuspended in 0.1% Glutaraldehyde, and a drop was mounted on an ion-coated copper grid supported by a carbon-coated film. The sample was stained with 1% uranyl acetate and visualized by TEM. Scale bar represents 100 nm. (C) Exosomal samples were captured by cryo-TEM. Vitrified unstained specimens were loaded to a Tecnai T12 G2, operating at 120 kV, and examined at a low dose to minimize radiation damage. The arrows point to iron cores. Scale bars represent 100 nm.